Report No. 167 / UILU ENG-94-4014

Crack Closure in Weldments

by

C. Y. Hou and F. V. Lawrence

A report of
MATERIALS ENGINEERING — MECHANICAL BEHAVIOR
College of Engineering, University of Illinois at Urbana-Champaign
October 1994

CRACK CLOSURE IN WELDMENTS

C. Y. Hou* and F. V. Lawrence†

*Department of Civil Engineering, 205 N. Mathews, University of Illinois, Urbana, IL 61801, U.S.A.

†Departments of Civil Engineering and Material Science and Engineering, 205 N. Mathews, Urbana, IL 61801, U.S.A.

Abstract

The strip-yield model for notched components (SYMNC model) which is based on Newman's model for crack closure was used to simulate the fatigue behavior of welded joints. A special finite element mesh was needed to estimate the loading-direction plastic stretches at the weld toe because of its asymmetrical shape. These notch-tip plastic stretches were combined with the crack-tip plastic stretches to estimate the effective stress-intensity factor ratio as a function of crack length. The predictions of the SYMNC model showed that the crack closure of a stress-relieved weldment is affected by the weld-toe plastic zone for the cases of stress ratio $R = 0$. The observed crack-closure behavior of an as-welded T-joint with residual stresses was also predicted using the SYMNC model.

Nomenclature

a	Crack length
C', m	Material constants for modified Paris law
da/dN	Crack growth rate
ε_p	Loading-direction plastic strain
f	Elastic crack-face displacement caused by unit remote load
g	Influence function in Newman's model
K_c	Fracture toughness
K_{max}, K_{min}	Applied maximum and minimum stress-intensity factor
K_{res}	Stress-intensity factor induced by residual stress
K_{Smax}	Stress intensity caused by maximum remote stress
L_i	Length of residual plastic stretches
R, R'	Stress ratio and effective stress ratio
r	Weld toe radius
ρ_c,ρ_n	Crack-tip and notch plastic zone size

S_{max}, S_{min}	Maximum and minimum remote stress
t	Base plate thickness of weldments
$U(a)$	Effective stress-intensity factor ratio, a function of crack length
u_{res}	Elastic crack-face displacement caused by residual stress
u_{Smax}	Elastic crack-face displacement caused by maximum remote stress
u_{σ}	Elastic crack-face displacement caused by strip-yield load
W	Plate width
$\Delta K'$, K'_{max}, K'_{min}	Stress intensities in residual stress field
ΔK, ΔK_{eff}	Stress-intensity range and effective stress-intensity range
S_y, S_u	Yield and ultimate strength of material

Crack Closure

The concept of crack closure [**1**] clarifies many puzzling fatigue-crack propagation phenomena which cannot be dealt with using the nominal range in stress intensity factor (ΔK). Crack closure diminishes the apparent crack-tip driving force. Correlating the crack growth rate with the effective stress intensity factor (ΔK_{eff}), the range in stress-intensity during which the crack is open, leads to a better crack-growth model which can deal with the behavior of short cracks, mean and residual stress effects, crack acceleration and retardation due to over and underloads:

$$da/dN = C'(\Delta K_{eff}(a))^m = C'(U(a)\Delta K(a))^m \quad (1)$$

To use Eq. 1 for fatigue life predictions, one must know $U(a)$ and $\Delta K(a)$. Finite element analysis (FEA) and the weight function concept are commonly used to calculate $\Delta K(a)$. However, the great difficulty in applying Eq. 1 to practical situations is estimating the effective stress-intensity factor ratio, $U(a)$.

A relatively simple numerical method for calculating the effective stress-intensity factor ratio $U(a)$ is the Dugdale strip-yield model as modified by Newman [**2,3**]. Newman's model estimates the crack-face contact stresses by calculating the magnitude of the plastic wake left behind the crack tip from which the crack-opening stresses and $U(a)$ can be estimated.

To estimate the crack-closure behavior of notched components, Hou and Lawrence [**4**] proposed a Strip-Yield Model for Notched Components (SYMNC) which considers the additional effects of notch-root plasticity (the notch plastic zone) by modifying Newman's strip-

yield model [2,3]. In the current study, the SYMNC model is used to estimate the crack closure in welded joints. A brief description of the SYMNC model is given in the Appendix.

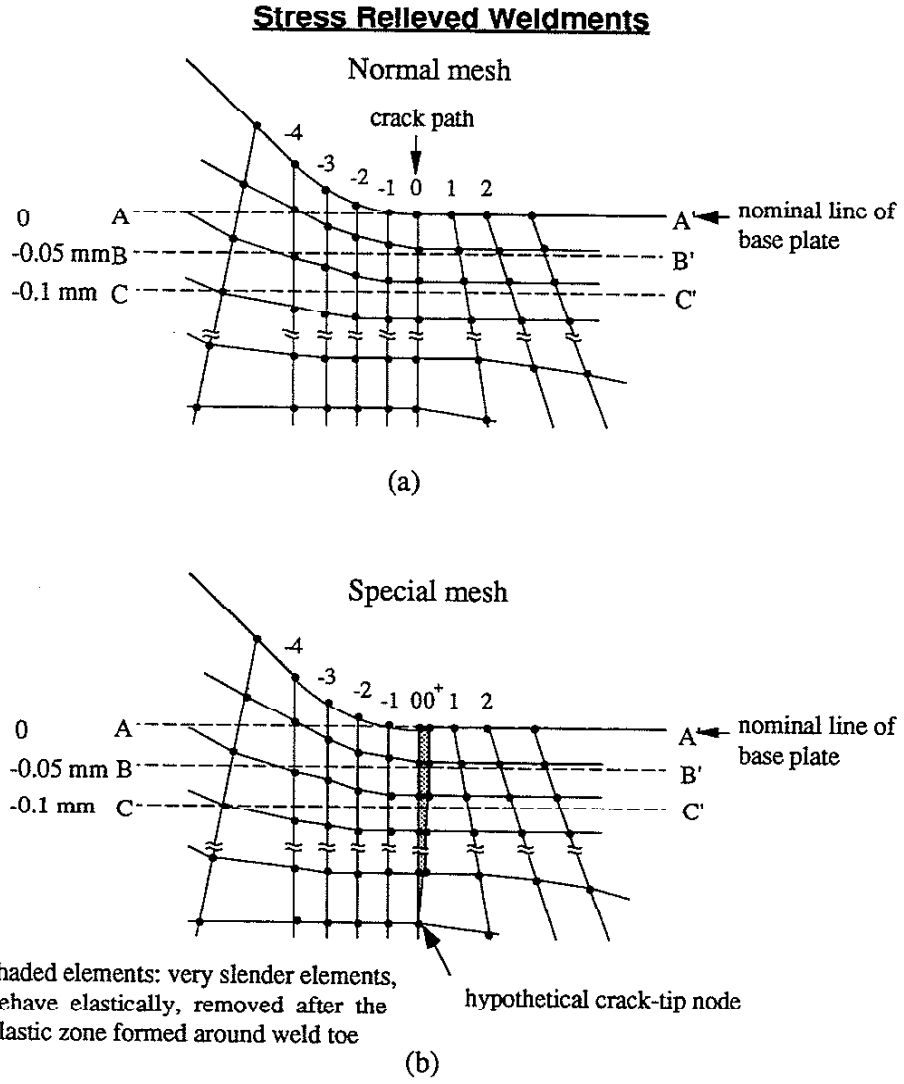

Fig. 1 Finite element meshes around a weld toe. (a) The normal mesh. (b) The special mesh.

A Special Finite Element Mesh for Determining Weld-Toe Plastic Stretches

To account for the influence of the weld-toe (notch root) plastic deformation on crack closure in weldments, a so called "two-notched-plates" procedure was used to calculate the weld-toe notch plastic stretches (NPS): see Appendix. However, unlike the symmetrically notched plates used in the (original) calculation of the NPS discussed in the Appendix, the path of a crack

which starts from a weld toe is not a plane of symmetry, that is, a line on which the finite element boundary condition nodes are located (see **Fig. 1**, the normal mesh). Therefore, the hypothetical crack of the first notched plate in the two-notched-plates procedure (Appendix) cannot be introduced by releasing boundary condition nodes in the weldment FEA.

Modifications have been made in the finite element mesh to make the procedure for the analysis of the NPS applicable to weldments. **Figure 1(a)** shows a normal finite element mesh around a weld toe. Assume that the hypothetical crack lies on the mesh line denoted as 0. Mesh lines on the right side of the crack line are denoted by ascending numbers and by descending numbers on the opposite side. An elastic-plastic FEA of this mesh can only give plastic strains around the weld toe. To obtain the notch-tip-plastic stretches (NPS), a mesh line (0^+) (see **Fig. 1(b)**, the special mesh) is inserted between line 0 and line 1. One of the ends of line 0^+ is located at the hypothetical crack tip which is an arbitrarily chosen element node on line 0 and is located beyond the weld-toe plastic zone. The other end is located at the nominal line of base plate and is a very small distance from the corresponding end of line 0. Every node on line 0 has a corresponding node on line 0^+. A series of very slender elements formed by the nodes on line 0 and line 0^+ are inserted. After being loaded to produce the weld-toe plastic zone, the hypothetical crack is introduced by removing these slender elements to produce a pair of crack-face displacements $u_{A0}(a_A,x)$ and $u_{A0^+}(a_A,x)$. The other weldment mesh with no elements inserted between line 0 and line 0^+ is loaded to obtain another pair of crack-face displacements $u_{B0}(a_A,x)$ and $u_{B0^+}(a_A,x)$. As discussed in the appendix, the difference between $u_{A0}(a_A,x)$ and $u_{B0}(a_A,x)$ and the difference between $u_{A0^+}(a_A,x)$ and $u_{B0^+}(a_A,x)$ are the weld-toe NPS on the two sides of the hypothetical crack, respectively.

Crack-closure behavior at a weld toe can be estimated by the SYMNC model using the calculated weld-toe NPS. It is important to note that the formulation of the strip-yield model and the described technique for obtaining weld-toe NPS assume 2-D through-thickness cracks. The use of the 2-D crack to estimate crack closure in weldments is an idealization since 3-D surface cracks are commonly observed in weldment fatigue tests.

Comparison of Predicted Results with the Experimental Data of Cruciform Weldments

Verreman and his coworkers [**5,6**] used strain gages to measure the crack lengths and crack-opening stresses of non-load carrying, GMAW cruciform joints. Uniform through-width cracks were observed in their tests, therefore, the experimental results can be used to verify the validity of the current 2-D SYMNC model for weldments. Since the residual stresses of the specimens were eliminated by heat treatment, residual stress effects on crack propagation were not considered in the predictions.

The base plate was ASTM A36 steel and the geometry of the weld are shown in **Fig. 2(a)**. **Table 1** shows the material properties required in the predictions. Four-node quadrilateral elements were used for the FEA of weld-toe NPS. The element formed between line 0 and line 0^+ at the hypothetical crack tip is not a quadrilateral element but is a constant-strain triangle element (see **Fig. 1(b)**). For simplicity, the lack of penetration was not modeled in the meshes. Figure 2(b) shows the meshes around the weld toe which was 50μm[1]. The line 0 and line 0^+ are so close (the distance between the top ends of these two lines was 0.1 μm) that they cannot be distinguished in the mesh.

Table 1 THE MATERIAL PROPERTIES OF THE STEELS CONSIDERED.

	S_y (MPa)	S_u (MPa)	C' *	m *
ASTM A36 steel	224	414		
JIS SM50A steel	330	510	1.0×10^{-8} **	3
As-welded T-joint	421	509		

*These values were obtained from experimental da/dN versus ΔK_{eff} curves given in the literature.
** The C' value listed is for da/dN in units of mm/cycle.

The special mesh is a substitute for the normal mesh for the NPS at weld toe. Since the NPS are related to loading-direction plastic strains, the monotonically loaded weld-toe plastic strains calculated from the special mesh without removing slender elements were compared with those obtained from the normal mesh to check the validity of the special mesh. The isotropic hardening rule and the von Mises yielding criterion were used in the elastic-plastic FEA. Because the slender elements in the special mesh caused divergent solutions if they were permitted to behave elastic-plastically, all the slender elements were forced to behave elastically by imposing a very high yield stess on them during the FEA calculation. Axial load levels of S_{max} = 147 and 177 MPa were applied. Loading-direction plastic strains at the intersections of mesh lines (line -4 to line 2) and the horizontal dash lines (AA', BB', CC') were calculated by interpolation of the plastic strain values at element nodes (see **Fig. 1**). Line AA' was coincident with the nominal line of base plate. Lines BB' and CC' were 0.05 and 0.1 mm below line AA',

[1]The weld toe radius was reported to be 50 μm or less. Verreman et al. also performed FEA for the weld-toe plastic zone based on both the cyclic and monotonic properties of base plate. They concluded that the crack-closure behavior was strongly affected by the size of the monotonic weld-toe plastic zone.

respectively. The node strains on line 0 of the normal mesh are presented by the corresponding node strains on line 0 and 0^+ in the special mesh, therefore, the average of the node plastic strains along line 0 and line 0^+ were compared with the corresponding plastic strains along line 0 calculated from the normal mesh.

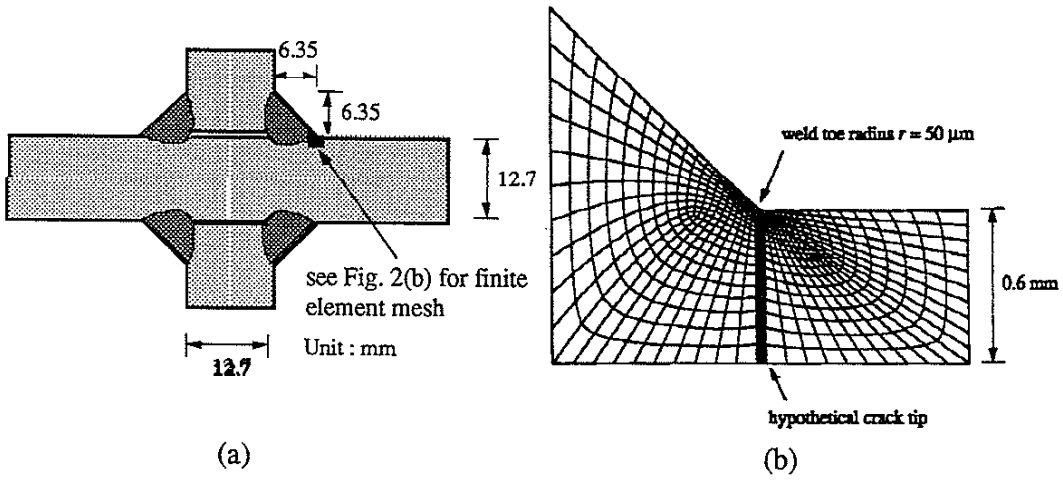

Fig. 2 The stress-relieved weld. (a) The geometry of the cruciform weldment. (b) The finite element mesh around the weld toe.

Figure 3 show the ratios of loading-direction plastic strain from the special mesh ($\varepsilon_{p,spe}$) to those from the normal mesh ($\varepsilon_{p,nor}$) of the two load levels. Almost all of the points where the plastic strains were recorded had ratio values of approximately unity except for a sudden drop along line 0. This result indicates that the presence of the slender elements in the special mesh caused a strain field discontinuity. Although the strain-field disturbance exists, the special mesh can still be used to calculate the plastic stretches at weld toe because the disturbance of strain field only occurs in a small locality around line 0 and line 0^+. Hence, the NPS calculated from the special mesh will be close to the NPS in the normal mesh.

Figure 4 show the calculated $u_{A0}(a_A,x)$, $u_{B0}(a_A,x)$, $u_{A0^+}(a_A,x)$ and $u_{B0^+}(a_A,x)$. The shaded area between $u_{A0}(a_A,x)$ and $u_{B0}(a_A,x)$, and the area between $u_{A0^+}(a_A,x)$ and $u_{B0^+}(a_A,x)$ are the weld-toe NPS on the both sides of the hypothetical crack. It is obvious that the calculated sizes of the two sets of NPS are different because the weld-toe plastic zone is not symmetric about the hypothetical crack line. Since the plastic stretches considered in the strip-yield model are symmetric about the crack line, the average of the calculated NPS on two sides of the hypothetical crack was adopted in the SYMNC model for estimating crack closure in the weld.

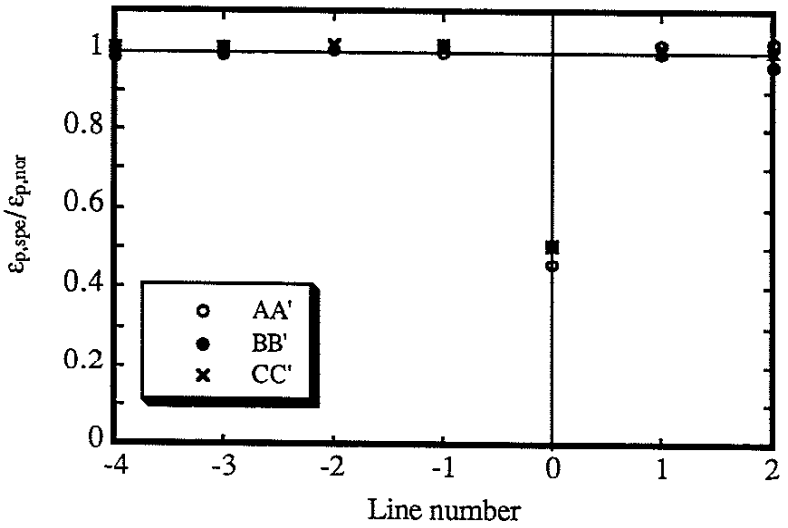

Fig. 3 The ratio of plastic strain calculated from the normal mesh and the special mesh.

Figure 5(a) shows the predicted $U(a)$ curves of the two stress levels (S_{max} = 147 and 177 MPa) at stress ratio R = 0. The crack closure caused by the weld-toe plastic zone causes the "dips" in the predictions. Apparently, the experimental data also show these "dips". For the stress ratio R = -1, the $U(a)$ curves of three stress levels (S_{max} = 118, 137, and 177 MPa) were calculated. The predicted results and the measured data are shown in Fig. 5(b). For the case of R = -1, no dips are observed in the U(a) curves because the compressive minimum stress of the (constant amplitude) load history eradicates the effect of the NPS on crack closure.

As-Welded Weldments

Residual stresses in weldments are caused by the non-uniform thermal distortions during the welding process. Any residual stress field must be in self-equilibrium, and the magnitude of maximum tensile component in weldments can be as high as the yield strength of base metal. It is known that residual stresses increase the mean stress and reduce the weldment fatigue strength. To estimate the crack closure of as-welded weldments, the residual stresses in the vicinity of the crack tip must be considered.

For cracks propagating in a residual stress field, Parker [7] proposed using the linear superposition principle to account for the additional stress intensity induced by residual stresses. The weight function method is commonly used to estimate the residual stress-intensity factor $K_{res}(a)$. When the $K_{res}(a)$ is introduced, the actual crack-tip driving forces during cyclic loading are:

$$K'_{max}(a) = K_{max}(a) + K_{res}(a)$$
$$K'_{min}(a) = K_{min}(a) + K_{res}(a) \quad (2)$$
$$\Delta K'(a) = K_{max}(a) - K_{min}(a) = \Delta K(a)$$

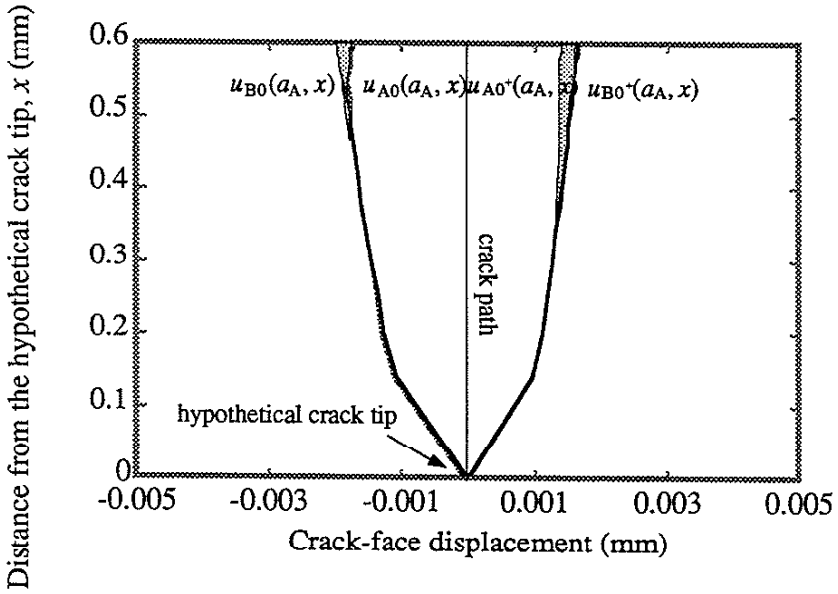

Fig. 4 The calculated weld-toe plastic stretches. S_{max} = 147 MPa.

However, the effective stress ratio R' varies as a function of crack length:

$$R'(a) = \frac{K'_{min}(a)}{K'_{max}(a)} \quad (3)$$

Glinka [8] observed the crack growth rate under various types of residual stress fields and found that tensile residual stresses increase the crack growth rate. As cracks propagate into the region of compressive residual stress, the test data approached and merged with the baseline data (crack growth rate obtained for plain plate without residual stresses). Glinka also used Forman's equation which considers the stress ratio R' effects to predict his experimental data:

$$\frac{da}{dN} = \frac{C\Delta K^m}{(1-R')K_c - \Delta K} \quad (4)$$

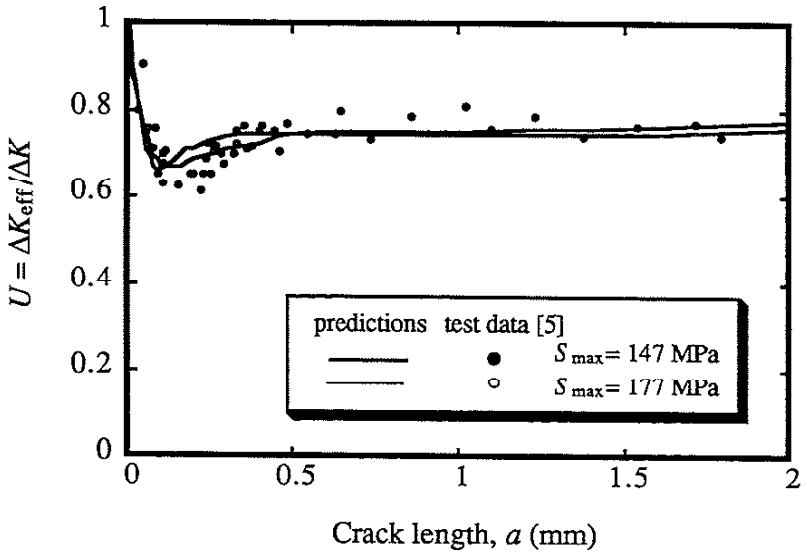

(a)

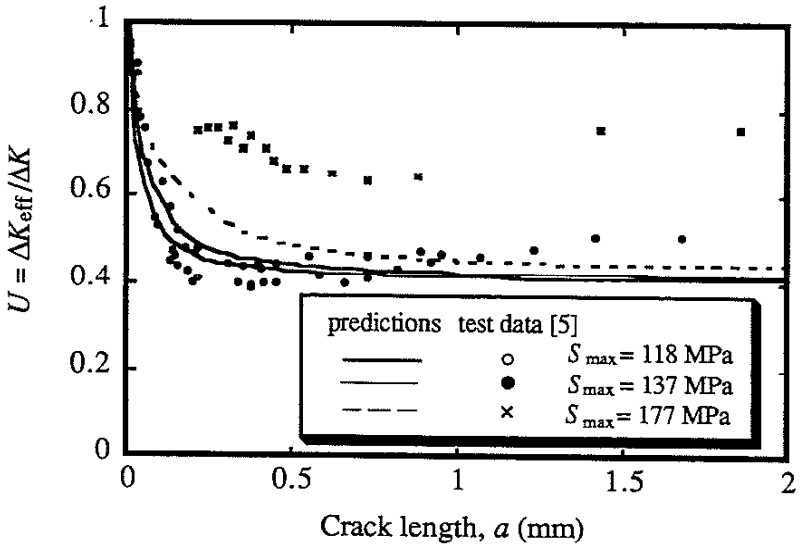

(b)

Fig. 5 The comparison of the predicted $U(a)$ curves with the test data. (a) $R = 0$. (b) $R = -1$.

where K_c is the fracture toughness. The predicted crack growth rate showed a sharp decrease for increasing ΔK which was not demonstrated by the experimental data.

Nelson [9] argued that this discrepancy was due to the superposition method used. Instead of using the superposition method, he tried to avoid this artificial effect by using the crack-closure concept. Ohta et al. [10] tested cracks propagating in weldment tensile residual field and found that crack closure occurred only under a high, compressive, external load. In a subsequent work, Ohta and coworkers [11] applied a two-step loading on a fatigue crack propagating in a tensile residual stress field. A constant stress-intensity range was first applied followed by another constant stress-intensity range loading. Transient crack growth rate is expected to be observed after changing the applied load level due to changes in the crack-closure level. However, no transient effects on crack growth behavior were observed because of the tensile residual stresses. Again, they concluded that no crack closure existed in weld tensile residual stress fields. Itoh et al. [12] and Kang et al. [13] studied the crack growth behavior influenced by residual stresses under various stress ratios. They both concluded that crack closure successfully correlated the test data.

Wang and Blom [14] first applied the Newman's strip-yield model to study the problem of crack closure in residual stress fields. They converted the $K_{res}(a)$ to an equivalent uniformly distributed remote load which induces the same value of $K_{res}(a)$ at crack tip. A total remote load (the sum of the applied remote load and the converted remote load) was then used to predict crack growth rate affected by residual stresses in a CT specimen.

Since the role played by residual stresses is the same as the role of mean stress (which can be explained by crack closure), the strip-yield model for crack closure is capable of predicting the crack propagation behavior in a residual stress field. In current study, the basic concept for considering the effects of residual stresses using the strip-yield model is similar to the superposition of the stress-intensity factors: see Eq. 2. However, instead of using a stress-intensity factor, crack-face displacements are superposed. A brief description of the approach of incorporating the residual stress effects in the strip-yield model is given in the Appendix.

Comparison of Predicted Results with the Test Data

Kang et al. [13] studied crack propagation in a tensile residual stress field and focused on the effects of negative R ratios. The cracks were oriented perpendicular to the weld. Because the initial crack tip (initial crack length a_i = 8 mm) was beyond the HAZ, the crack propagation behavior was not affected by the microstructural differences between the base metal and the HAZ and was only affected by the residual stresses. The specimen, the crack geometries, and the shape of the measured residual stress distribution are shown in **Fig. 6**. The $K_{res}(a)$ was calculated using the following equation with the residual stress distribution given in their paper:

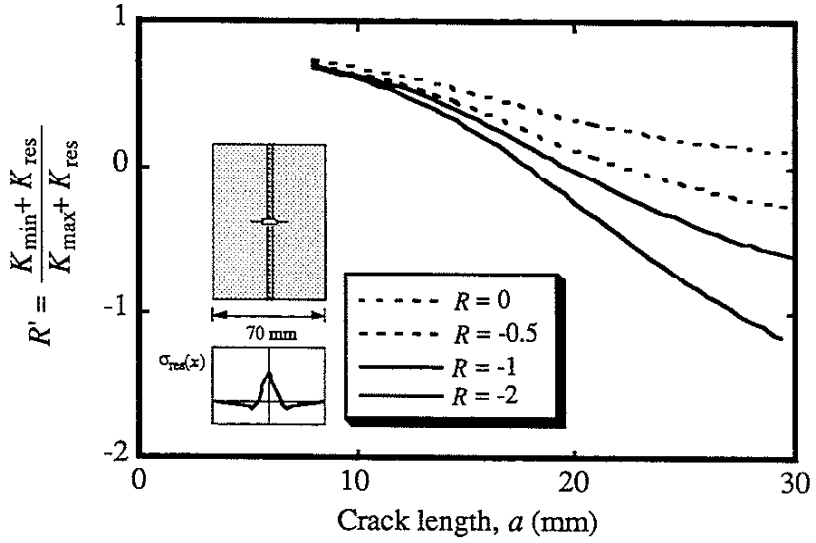

(a)

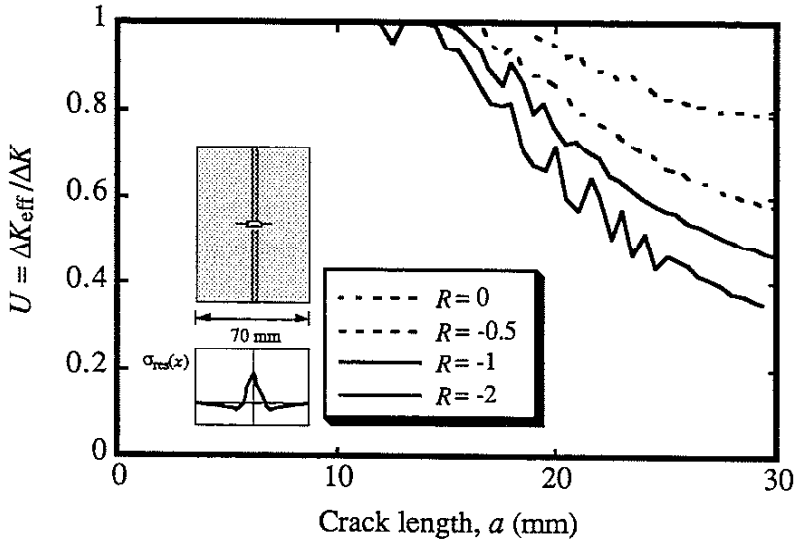

(b)

Fig. 6 The crack propagation behavior in a residual stress field. (a) the R' values (b) the U values.

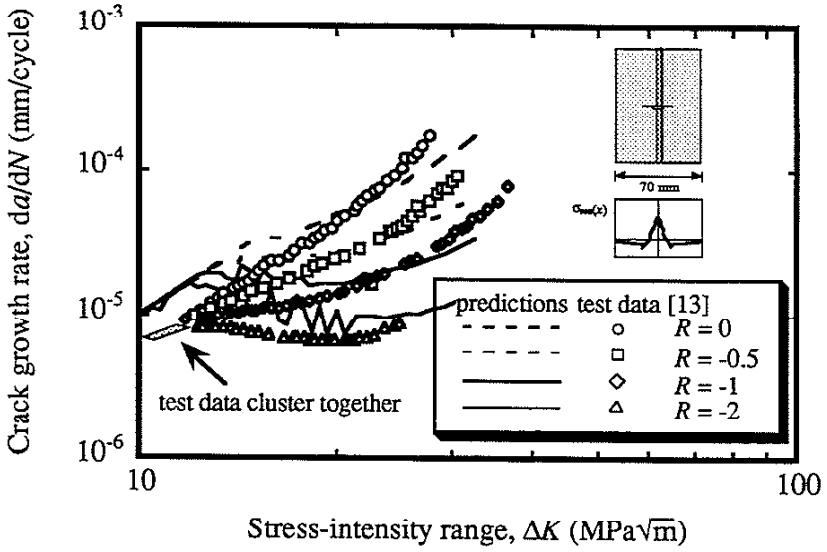

(c)

Fig. 6 (cont.) The crack propagation behavior in a residual stress field. (c) the crack growth rates.

$$K_{res}(a) = \int_{-a}^{a} \sigma_{res}(x) \left[\frac{2\sin\frac{\pi(a+x)}{W}}{W\sin\frac{2\pi a}{W}\sin\frac{\pi(a-x)}{W}} \right]^{1/2} dx \qquad (5)$$

The base metal was JIS SM50A steel. The thickness of the specimen was 6 mm. The mechanical properties and the constants for the modified Paris equation of this steel are listed in Table 1. The applied stress ratio ranged from $R = 0$ to $R = -\infty$. Because the applied stress levels were not given explicitly in the paper, this information was obtained by converting the given $K_{max} + K_{res}$ versus crack length relationship to the applied stress levels. The results showed that S_{max} was 50, 33.3, 25, and 16.7 MPa for stress ratio $R = 0$, -0.5, -1, and -2, respectively.

The calculated R' using Eq. 3 is shown in **Fig. 6(a)**. Initially, cracks propagate in tensile residual stress region. The values of R' are strongly affected by the residual stress field, and all the values cluster at 0.65 to 0.75 despite the fact that the nominal R values ranged from -2 to 0. At these high effective stress ratios, little crack closure or even no crack closure should be expected since it is well known that cracks tested at high nominal stress ratios (without residual stresses) exhibit no crack-closure effects. As cracks become longer, the effects of residual stresses decrease and the values of R' approach their nominal R values. **Figure 6(b)** shows the predicted $U(a)$ curves. Note that the U values are initially unity which correspond to high R'

values, that is, no crack closure occurs. As cracks propagate a distance, the U values start to decrease indicating the occurrence of crack closure. This distance is dependent on the nominal R values. For more negative nominal R values, crack closure takes place at a shorter crack length. Figure 6(c) shows the predicted and observed crack growth rate at various nominal R ratios. The test data cluster when nominal $\Delta K < 13$ MPa$\sqrt{\text{m}}$ indicating that the crack growth rate is independent of the nominal R values. This trend indicates that no crack closure exists, i.e., no crack-tip driving forces reduction occurs at the crack tip. Therefore, all cracks tested at various R values are subjected to the same ΔK_{eff} (which equals the nominal ΔK) and show the same crack growth rate. However, as the cracks become longer and crack closure takes place, the crack growth rates separate and show the known effects of stress ratio (R) on da/dN versus ΔK. Apparently, the predicted crack growth rate shows the same trend as the experimental data.

Comparison of Predicted Results with the Test Data of an As-Welded T-Joint

Unlike a well-defined notch, the measurement of crack closure in a welded joint is much more difficult because the locations where surface cracks start are not known at the start of the test. Furthermore, many accurate techniques for crack closure measurement, such as crack-tip strain gauge and crack-tip clip gauge, are not easily applied to welded joints.

When one applies the crack-closure concept to the fatigue life prediction of weldments, residual stresses must be considered. **Figure 7** shows the loading-direction residual stress distributions parallel and transverse to a weld. It is obvious that if a crack is initiated at weld toe close to the center of the plate (location A), the crack is fully embedded in a tensile residual stress field which will easily open the crack; hence, crack closure is unlikely to develop under this condition. Of course, residual stress relaxation could decrease these tensile residual stress and create an environment for the development of crack closure. As the crack propagates into a compressive residual stress field, crack closure is certain. If the crack starts from a location close to the edge of the plate, i.e., location B, which is in the compressive stress field of the residual stress distribution parallel to the weld, the compressive residual stresses reduce the nominal R values and will induce crack closure in the early stage of crack propagation.

It has been shown that crack closure in a weld is affected by both the weld-toe plastic zone and the residual stresses. The numerical techniques to solve these weld-toe plastic zone and residual stress problems have been developed separately and will be combined to predict crack closure in an as-welded joint.

Otegui, Mohaupt and Burns [**15**] placed ten strain gauges close to the weld toe of a welded T-joint to detect crack initiation and early crack growth. These strain gauges were also used to measure the crack closure. The geometry of the T-joint is shown in **Fig. 8**. The average flank angle and weld toe radius were reported to be 40° and 0.5 mm. The mechanical properties

of base plate are listed in Table 1 and were used in the predictions. The applied bending stress range was 305 MPa at stress ratio $R = 0.1$.

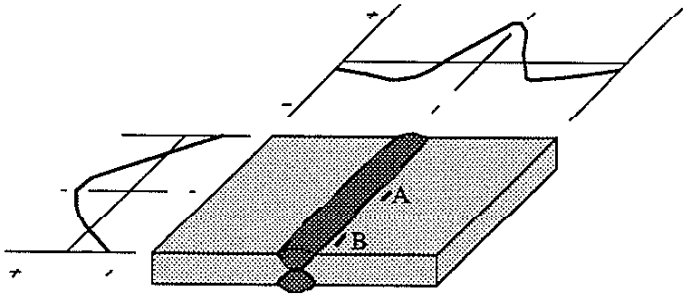

Fig. 7 The residual stress distributions in a welded plate.

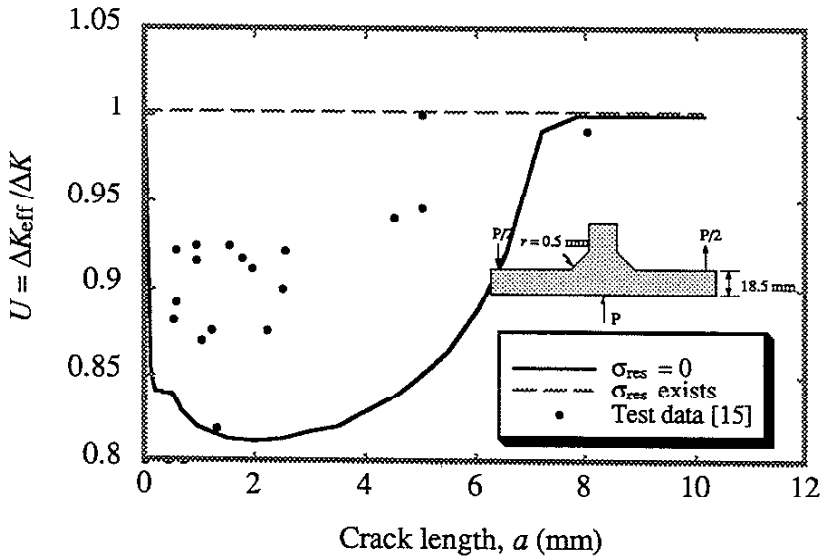

Fig. 8 The measured and the predicted crack closure effects for an as-welded T-joint.

Because the residual stress distribution is complex in a weld, a simple shape of the residual stress along the base plate thickness direction was assumed:

$$\sigma_{res}(x) = S_y \cos(\frac{2\pi x}{t}) \tag{6}$$

where t is the base plate thickness. Although tensile residual stress as large as the yield strength of the base plate was assumed as the worst case for weldments, Otegui et al. stated that the maximum tensile residual stress at the weld toe should range from one third to one half of the base metal yield strength. Therefore, 42% of S_y was used in Eq. 6 instead of S_y.

FEA results showed that the weld-toe monotonic plastic zone size was approximate 0.45 mm.

Crack closure both with and without residual stress was calculated. **Figure 8** shows that no crack closure was predicted when the welding residual stresses were considered. The scatter in the measured data reflects the difficulties in measuring crack closure in a weld. It is obvious that most of the measured crack closure data were bounded by the two predicted curves.

Conclusions

1. A special finite element mesh was developed which can be used to estimate the plastic stretches around an asymmetrical notch such as a weld toe. Using these calculated weld-toe plastic stretches, the SYMNC model offers a simple and efficient numerical approach for calculating crack-closure in weldments.
2. The weld tensile residual stresses were found to increase the mean stress effect, and hence, reduce the crack-closure levels. The crack-closure behavior of an as-welded joint is complicated by the fact that the crack initiation sites are unknown and the residual stress distributions are uncertain. However, most of the measured U values of an as-welded weldments were bounded by the predicted results of the SYMNC model considering: (1) no residual stress, and (2) $U(a) = 1$.

Acknowledgments

This investigation was supported by the Fracture Control Program at the University of Illinois at Urbana-Champaign and the Cooperative Research Program at Edison Welding Institute. The authors wish to thank Dr. J. C. Newman, Jr. and Prof. H. Sehitoglu for many useful discussions. Ms. Nong Chen kindly read the paper and made many helpful suggestions.

References

1. W. Elber (1971) The Significance of Fatigue Crack Closure. In *Damage Tolerance in Aircraft Structure, ASTM STP 486*, pp. 230-242.
2. J. C. Newman, Jr. (1983) A Crack-Closure Model for Predicting Fatigue Crack Growth Under Aircraft Spectrum Loading. In *Methods and Models for Predicting Fatigue Crack Growth Under Random Loading, ASTM STP 748*, pp. 53-84.
3. J. C. Newman, Jr. (1983) A Nonlinear Fracture Mechanics Approach to the Growth of Small Cracks, *AGARD Report 328*, pp. 6.1-6.26.

4. C. Y. Hou and F. V. Lawrence, A Crack-Closure Model for the Fatigue Behavior of Notched Components. Accepted by *ASTM STP Advances in Fatigue Lifetime Predictive Techniques*.
5. Y. Verreman, J.-P. Baïlon and J. Masounave (1987) Closure and Propagation Behavior of Short Fatigue Cracks at Different R-Ratios. In *Fatigue 87*, pp. 371-380.
6. Y. Verreman, J.-P. Baïlon and J. Masounave (1987) Fatigue Life Prediction of Welded Joints - A Re-Assessment. *Fatigue Fract. Engng. Mater. Struct.*, **10**, 17-36.
7. A. P. Parker (1982) Stress Intensity Factors, Crack Profiles, and Fatigue Crack Growth Rates in Residual Stress Fields. In *Residual Stress Effects in Fatigue, ASTM STP 776*, pp. 13-31.
8. G. Glinka (1979) Effect of Residual Stresses on Fatigue Crack Growth in Steel Weldments Under Constant and Variable Amplitude Loads. In *Fracture Mechanics, ASTM STP 677*, pp. 198-214.
9. D. V. Nelson (1982) Effects of Residual Stress on Fatigue Crack Propagation. In *Residual Stress Effects in Fatigue, ASTM STP 776*, pp. 172-194.
10. A. Ohta, M. Kosuge, T. Mawari and S. Nishijima (1988) Fatigue Crack Propagation in Tensile Residual Stress Fields of Welded Joints Under Fully Compressive Cycling. *International Journal of Fatigue*, **10**, 237-242.
11. A. Ohta, A. J. McEvily and N. Suzuki (1993) Fatigue Crack Propagation in a Tensile Residual Stress Field Under a Two-Step Programmed Test. *International Journal of Fatigue*, **15**, 9-12.
12. Y. Z. Itoh, S. Suruga and H. Kashiwaya (1989) Prediction of Fatigue Crack Growth Rate in Welding Residual Stress Field. *Engineering Fracture Mechanics*, **33**, 397-407.
13. K. J. Kang, J. H. Song and Y. Y. Earmme (1989) Fatigue Crack Growth and Closure Through a Tensile Residual Stress Field Under Compressive Applied Loading. *Fatigue Fract. Engng. Mater. Struct.*, **12**, 363-376.
14. G. S. Wang and A. F. Blom (1991) A Strip Model for Fatigue Crack Growth Predictions Under General Load Conditions. *Engineering Fracture Mechanics*, **40**, 507-533.
15. J. L. Otegui, U. H. Mohaupt and D. J. Burns (1991) Effect of Welded Process on Early Growth of Fatigue Cracks in Steel T Joints. *International Journal of Fatigue*, **13**, 45-58.

Appendix

The SYMNC model

Newman's original strip-yield model calculates crack-closure effects by considering only the loading-direction crack-tip plastic deformation (or crack-tip plastic stretches, CTPS). Hou and Lawrence [4] modified Newman's original formulation to adapt this model for cracks emanating from various notches. It was found that the plastic wake left behind the crack tip is mainly due to the notch plastic stretches (NPS, which are produced by notch plastic deformation) when crack length is small compared with notch plastic zone size. Hence, the NPS should be incorporated into the Newman's original strip-yield model. The "two-notched-plates" procedure used to determine the magnitude of the NPS is described below.

First consider a notched plate (Fig. A.1) loaded by a remote load S which induces a notch plastic zone: see Fig. A.1(a). Next, a crack of length a_A is introduced: see Fig. A.1(b). The introduction of this hypothetical crack would result in crack-face displacements $u_{nA}(a_A,x)$: see Fig. A.1(c). Now, consider a second notched plate having a preexisting crack of the same length: see Fig. A.2(a). This second notched plate is then loaded by remote stress S ; however, a different set of crack-face displacements $u_{nB}(a_A,x)$ would result: see (Fig. A.2(b)). The NPS as a function of the distance from the notch root (x) is:

$$\frac{\mathrm{NPS}(x)}{2} = u_{nB}(a_A,x) - u_{nA}(a_A,x) \qquad \text{(A.1)}$$

This procedure can be carried out by performing an elastic-plastic FEA. Since the plates are symmetrical about the crack path, the hypothetical crack in the first plate can be introduced by releasing the element nodes which are located on the crack path, i. e., boundary condition nodes.

The calculated CTPS (from the theory of Dugdale-type crack) and the NPS (from the results of FEA) are linearly superposed together to form the total plastic stretches (TPS) in the plastic zone:

$$\mathrm{TPS} = \mathrm{NPS} + \mathrm{CTPS} \qquad \text{(A.2)}$$

The calculated TPS are used in the strip-yield model with the appropriate plastic zone size ahead of crack tip[2] to estimate the crack-closure behavior of a fatigue crack emanating from a notch root.

---

[2]When a fatigue crack-tip plastic zone is entirely embedded in a notch plastic zone, the plastic zone size used in the strip-yield model is notch plastic zone size (ρ_n, from FEA). For those cases in which the entire or part of the crack-tip plastic zone is located beyond the notch plastic zone, the crack-tip plastic zone size (ρ_c, from the theory of Dugdale-type crack) is used.

Including Residual Stress Effects in the Strip-Yield Model

The basic concept for considering the effects of residual stresses using the strip-yield model is similar to the superposition of the stress-intensity factors: see Eq. 2. However, instead of using a stress-intensity factor, crack-face displacements are superposed since the strip-yield model calculates crack closure based on crack-face displacements when the remote load is maximum and minimum (see Ref. 2 for details).

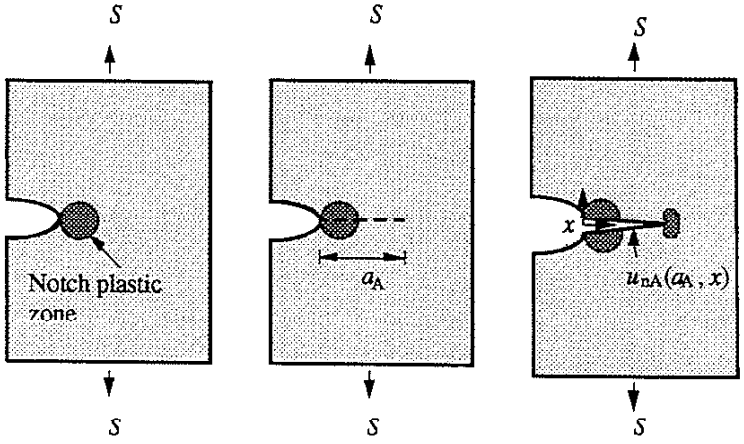

Fig. A.1 The notched plate for $u_{nA}(a_A, x)$.

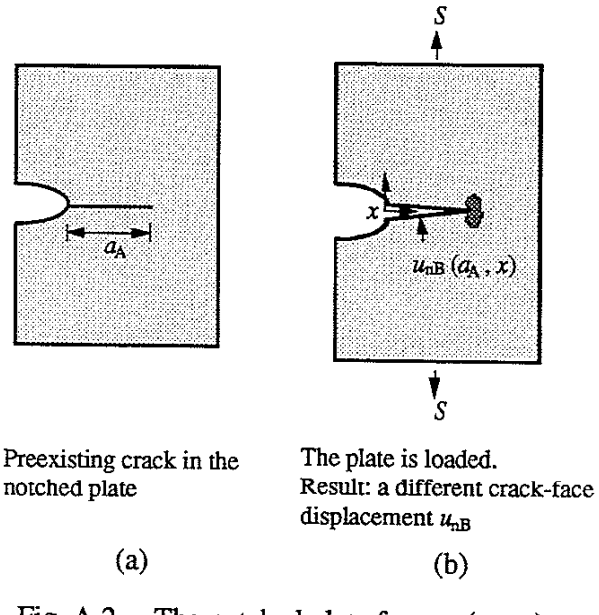

Fig. A.2 The notched plate for $u_{nB}(a_A, x)$.

Fig. A.3 shows a Dugdale-type crack in a residual stress field. This elastic-plastic crack (Fig. A.3(a)) can be analyzed by superposing two fictitious elastic cracks (Fig. A.3(b) and (c)). The crack-tip plastic zone (ρ_c) at maximum load can be obtained by:

$$K_{Smax} + K_{res} = K_{\sigma} \tag{A.3}$$

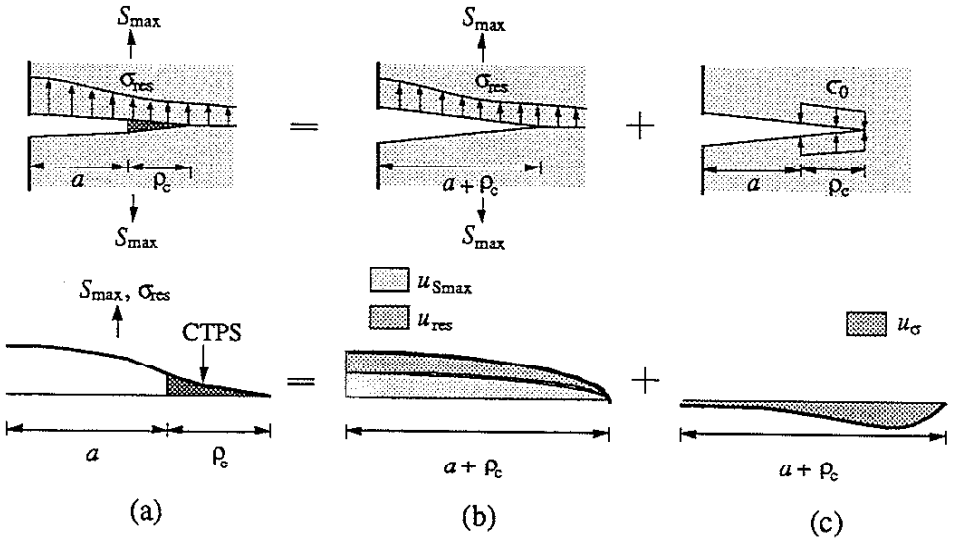

Fig. A.3 A Dugdale-type crack in a residual stress field.

The magnitude of CTPS in the range from a to $a+\rho_c$ can be obtained by superposing three elastic crack-face displacements:

$$\text{CTPS}(x) = u_{Smax}(x) + u_{res}(x) + u_{\sigma}(x) \quad \text{for } a < x < a+\rho_c \tag{A.4}$$

The calculated CTPS are incorporated with the NPS (from FEA) in the SYMNC model. When the crack is unloaded, the unloaded stresses in the plastic zone and the contact stresses along crack faces are calculated by the compatibility of the residual plastic deformation (see Ref. 2 for details):

$$\sum_{j=1}^{n} \sigma_j \, g(x_i, x_j) = S\, f(x_i) - L_i + u_{res}(x_i) \tag{A.5}$$

At minimum load, the residual length of the compressively yielded plastic stretches is calculated by:

$$I_i = S_{\min} f(x_i) - \sum_{j=1}^{n} \sigma_j \, g(x_i, x_j) + u_{res}(x_i) \qquad (A.6)$$

Note that when the calculated crack-tip plastic zone is entirely embedded in a notch plastic zone, the notch plastic zone size is used as the plastic zone size ahead of crack tip according the SYMNC model. Hence, the $f(x_i)$, $g(x_i,x_j)$,$u_{res}(x_i)$ in Eq. A.5 and A.6 are calculated using a fictitious crack length of $a+\rho_n$.